2008 IEEE International Conference on
Robotics and Automation
Pasadena, CA, USA, May 19-23, 2008

Kinematic Motion Control of Wheeled Mobile Robots Considering Curvature Constraints

Youngshik Kim, *Student Member, IEEE* and Mark A. Minor, *Member, IEEE*

Abstract— **This paper presents a time invariant kinematic motion controller for wheeled mobile robots. A *path manifold* that considers curvature limitations is used to provide a desired path shape and convergence to the reference posture or trajectory. Lyapunov based techniques are then used to derive a control law that asymptotically converges the robot to the *path manifold.* Posture regulation, path following, and trajectory tracking capability are provided. Allowable initial conditions are estimated based upon curvature constraints of the robot. Curvature boundaries and asymptotic convergence naturally limit allowable initial conditions and are resolved by driving the robot to intermediate goal points within regions of allowable initial conditions. The proposed controller is evaluated in simulation.**

I. Introduction

The subject of this research is a kinematic motion control law for wheeled mobile robots subject to physical constraints. Achievable path curvature is limited by physical design and dynamic effects. Most kinematic motion controllers have ignored these physical effects, though, and have focused solely on control and planning considering nonholonomic constraints. It is, however, important to include physical considerations in the kinematic motion controller since these commands are typically used as inputs to the dynamic controller of the physical system [1]. Thus, the goal of this research is to provide a single kinematic motion control law capable of all three motion control tasks while considering physical constraints. Our controller can provide this capability given particular regions of initial conditions and references with constrained velocity and curvature.

In order to satisfy velocity and curvature limitations while performing all three motion control tasks, we first embed curvature constraints in the controller using a *path manifold*. The *path manifold* is a geometric tool that defines the shape of the path that the robot follows while converging to its target or trajectory. In this case a circular *path manifold* with radius satisfying curvature constraints is used. The robot is driven to the *path manifold* using Lyapunov based control design. Once the robot reaches a neighborhood of the *path manifold* in finite time, velocity and curvature limitations are satisfied for posture regulation and for sufficiently constrained reference paths and trajectories. However, controller commands during convergence to the *path manifold* critically depend upon initial conditions and path/trajectory properties. Initial conditions in immediate proximity to the target are limited by curvature constraints, but this can be easily resolved by providing intermediate target configurations within allowable regions. We then demonstrate that this time invariant controller provides smooth bounded commands for motion control tasks given allowable initial conditions and constrained path/trajectory properties.

In previous research [2], a kinematic controller was derived in polar representation using the *path manifold* and Lyapunov based techniques. However, this controller becomes singular for some particular initial conditions, which should be avoided. This research presents a new *path manifold* based controller that resolves this singularity issue. Thus, a major contribution of this paper is a nonsingular kinematic motion controller that solves all three motion control tasks while considering curvature limitations given allowable initial conditions.

In Sec. II we compare our contributions to existing work. The general kinematics are derived in Sec. III. The *path manifold* is presented in Sec. IV and combined with Lyapunov functions to derive the control law in Sec. V. The control strategy is evaluated and discussed in Sec. VI. Concluding remarks are in Sec. VIII.

II. Background

Kinematic control of mobile robotic systems has received a great deal of attention in recent years and many motion control schemes have been proposed to consider their nonholonomic constraints. Traditionally, Cartesian coordinates have been used to model and control mobile robots [3, 4], but these efforts have resulted in discontinuous or time varying control laws. This is because a smooth time invariant control law cannot be realized to stabilize nonholonomic robots in Cartesian coordinates as proven by Brockett [5].

It is important to note that Brockett's theorem [5] requires a system to be continuous in a neighborhood of the equilibrium point. Thus, by introducing discontinuity in the equilibrium point with a polar coordinate system, Brockett's theorem

Manuscript received September 14, 2007. This work was supported by the National Science Foundation under Grant # IIS-0308056.

Youngshik Kim is a doctoral candidate at the University of Utah, Mechanical Engineering, Salt Lake City, UT 84112 USA (e-mail: youngshik.kim@utah.edu).

Mark. A. Minor is with the University of Utah, Mechanical Engineering, Salt Lake City, UT 84112 USA (phone: 801-587-7771; fax: 801-585-9826; e-mail: minor@mech.utah.edu).

cannot be applied and a smooth time invariant control law is allowed [6, 7]. Polar coordinates were applied to derive smooth and globally stabilizing state feedback control laws [7, 8]. Singularity occurs at the origin in the polar coordinate system. Singularity issues can be avoided by appropriately selecting initial conditions or intermediate points, or by applying a simple state feedback control law to make the closed loop system nonsingular [8]. Thus, the polar representation has been frequently adopted for posture regulation.

Path curvature is generally an issue for mobile robots given steering restrictions determined by mechanical design and traction limitations [9]. As shown in Fig. 1, it is assumed that permissible steering paths are restricted. Actuators likewise possess limited capabilities and realizable wheel velocity is restricted. Furthermore, excessive velocity commands may cause wheel slip, large path curvature, or excessive traction forces. Thus, saturation functions have typically been used to provide bounded velocity inputs in motion control. However, curvature constraints cannot be satisfied by simply saturating velocities. Further, velocity and curvature constraints have been considered by using saturation and designing control gains, respectively, for posture regulation [10]. However, aforementioned research does not provide path following or trajectory tracking capability.

In contrast to motion control, appreciable motion planning research has considered physical constraints on velocity and path curvature to provide feasible references [11]. In particular, arcs or circles have popularly been applied to construct a path due to their simplicity and bounded curvature [12]. Most notably, though, we consider these constraints in kinematic motion control as opposed to path planning. This helps to assure that the robot does not violate physical constraints while converging to its reference, as opposed to motion planning that focuses on assuring that the path itself is mindful of constraints.

The *path manifold* is a smooth path that a robot posture can be regulated along while satisfying curvature constraints. The *path manifold* has similarity to the sliding surface in sliding mode control in that the system variables converge to the equilibrium point along this manifold using a controller derived using Lyapunov based techniques. However, this research proposes a smooth and continuous kinematic controller based on ideal kinematics without the switching characteristic of sliding mode control. Thus, our kinematic controller provides smooth velocity references that can be used as inputs to a dynamic controller [1]. Sliding mode controllers have been used previously in dynamic motion controllers, but these have been used to track ideal velocity commands provided by kinematic motion controllers [13] and to track gradient lines of a potential field for obstacle avoidance [14].

The *path manifold* also provides uniform coordinates for the primary motion control tasks in error coordinates.

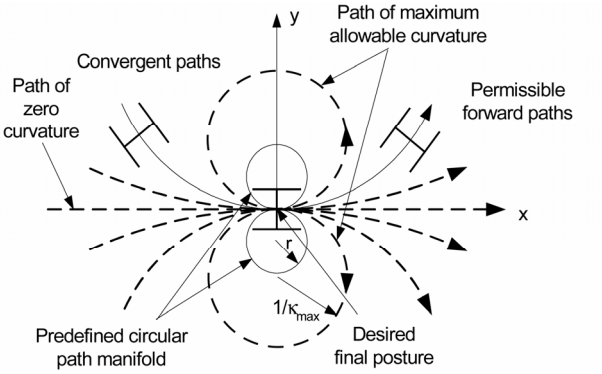

Fig. 1. Permissible forward paths and convergent paths of a mobile robot with respect to the path curvature.

Previously, we demonstrated the *path manifold* concept in [2] to realize bounded path curvature in the primary motion control problems with a single control law. However, the subsequently derived controller should be modified slightly to remove unacceptable singularities. In this research a new controller is derived to resolve this singularity issue using a new Lyapunov function and the *path manifold*. As a result, the controller presented here eliminates potential singularity caused by some particular initial conditions. Further, the controller expression is simpler, which reduces required computational loads.

III. KINEMATIC MODEL

In this section general kinematics of a unicycle type robot are presented based upon the polar representation. To consider the primary motion control tasks simultaneously, the reference posture is denoted using the reference frame *R*, Fig. 2. Note that the reference frame *R* represents a virtual reference posture such that it may describe the primary motion control tasks simultaneously. For posture regulation, the frame *R* is fixed in the global frame *G*. For path following, the frame *R* moves along a predefined geometric path consisting of the locus of positions and orientations. Arbitrary, but bounded, velocities can thus be chosen for the reference.

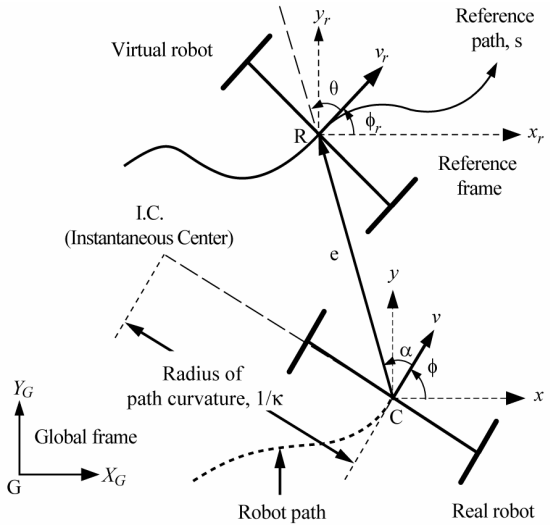

Fig. 2. Kinematics of a unicycle type mobile robot.

Further, for trajectory tracking, both trajectories of the frame R and the desired path are identically parameterized by time such that velocities are specified at each position. Thus, by simply modifying reference velocity expressions, the trajectory tracking controller may easily solve all primary motion control tasks. The reference posture is described using a virtual robot that inherits kinematics of the real robot such that it provides reference paths or trajectories that the robot can follow.

Using the polar representation relative to posture O, Fig. 2, the kinematics can be written in error coordinates,

$$\begin{aligned} \dot{e} &= -v\cos\alpha + v_r\cos\theta \\ \dot{\theta} &= v\frac{\sin\alpha}{e} - v_r\frac{\sin\theta}{e} - \dot{\phi}_r \\ \dot{\alpha} &= v\frac{\sin\alpha}{e} - v_r\frac{\sin\theta}{e} - \dot{\phi} \end{aligned}, \qquad (1)$$

where the angular velocity of point O can be described as a function of the path curvature, κ, and the linear velocity, v, such that $\dot{\phi} = v\kappa$. Likewise, the reference angular velocity is expressed as $\dot{\phi}_r = v_r\kappa_r$. The error states in polar representation are defined as,

$$\begin{aligned} e &= \sqrt{(x-x_r)^2 + (y-y_r)^2} \\ \theta &= ATAN2\left(-(y-y_r), -(x-x_r)\right) - \phi_r \\ \alpha &= \theta - \phi + \phi_r \end{aligned}. \qquad (2)$$

where x and y are the Cartesian coordinates of a moving coordinate frame attached to the point O. A reference position (x_r, y_r) is attached to the moving frame R to describe its location relative to the global frame G. The variable v represents the velocity of the coordinate frame O moving in a heading ϕ relative to the global frame G. The subscript r denotes the reference frame. Thus, v_r and ϕ_r are the reference velocity and the reference heading angle of the coordinate frame R, respectively. In this research, we focus on forward motion along smooth paths such that $v_r \geq 0$.

The path following and trajectory tracking problems can be solved by applying traditional nonlinear techniques to (1). However, traditional tracking controllers lack the ability to stabilize the robot to the desired posture when the reference coordinates are fixed (*i.e.* posture regulation). For this reason, posture regulation and reference tracking have traditionally been considered as different problems. However, these motion control problems can be solved simultaneously by using a *path manifold* that guides robot motion to the posture or target along a smooth path while satisfying curvature limitations.

IV. The Path Manifold

The *path manifold* specifies path shape during convergence to a desired posture or trajectory. In this research a circular *path manifold* is defined to satisfy curvature constraints. The *path manifold* is then applied to the kinematic equations to derive velocity expressions that assure stabilization along the manifold.

To realize a circular *path manifold*, Fig. 3, position and angle conditions are derived first. Position error in the coordinate frame of the reference is determined by,

$$\hat{x}_e = \hat{x}_r - \hat{x} = r\sin 2\theta,\ \hat{y}_e = \hat{y}_r - \hat{y} = r - r\cos 2\theta \ , \qquad (3)$$

where r is the radius of the circular *path manifold*. Applying (3) to the error definition (2), the position e is defined as, $e = \sqrt{(r\sin 2\theta)^2 + (r - r\cos 2\theta)^2} = r\sqrt{2}\sqrt{1-\cos 2\theta}$ where requirements for θ can be deduced from Fig. 3. Note that the velocity vector **v** and reference velocity vector $\mathbf{v_r}$ are tangent to Circles I and II. The position error vector **e** bisects the angle between **v** and $\mathbf{v_r}$ such that the angle α is equal and opposite of θ on the manifold. Denoting $\eta = \sqrt{1-\cos 2\theta} \geq 0$, the circular *path manifold* is thus,

$$e = \sqrt{2}r\eta,\ \alpha = -\theta \, . \qquad (4)$$

Several features of the circular *path manifold* are noted. First, since the *path manifold* is tangential to the $\hat{X}_r$ axis, this results in $\theta = \alpha = 0$ at the reference origin. Second, considering curvature constraints, we also have $r \geq r_{\min} = 1/\kappa_{\max}$. In particular, we choose $r = 1/\kappa_{\max}$ in this paper to demonstrate steering capability using maximum curvature. Finally, the circular *path manifold* selected depends upon initial orientation, $\theta(0)$: Circle I for $0 \leq \theta(0) \leq \pi$ and Circle II for $-\pi \leq \theta(0) < 0$, Fig. 3. Thus, paths generated by Circles I and II are symmetric with respect to the $\hat{X}_r$ axis since Circles I and II are so.

We now show that velocities can be calculated to assure convergence of the error state equations (1) along the *path manifold*. Differentiating (4) and comparing with (1), velocity expressions are,

$$v = v_r + 2r|\dot{\theta}|,\ \dot{\phi} = 2\dot{\theta} + \dot{\phi}_r \, , \qquad (5)$$

which provides stabilization along the *path manifold* given v_r and $\dot{\phi}_r$. Thus, these velocities drive the robot to the origin along a circular path such that (e, θ, α) converge to zero.

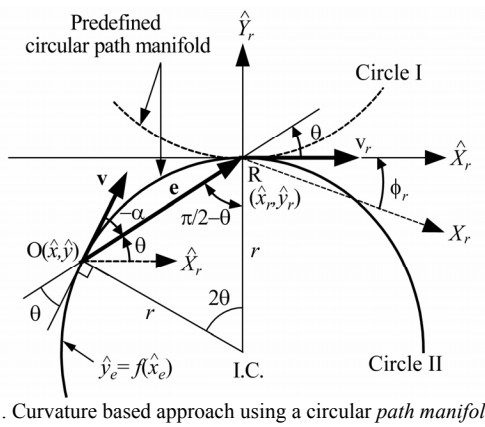

Fig. 3. Curvature based approach using a circular *path manifold.*

Once at the origin, (5) gives $v = v_r$ and $\dot{\phi} = \dot{\phi}_r$ such that $\dot{e} = \dot{\theta} = \dot{\alpha} = 0$. The origin of the error coordinates is thus an equilibrium point for trajectory tracking and path following as well as posture regulation.

V. Control Law

We now derive a motion controller that will drive the robot to the *path manifold*, which then steers the error coordinates to their origin. As a result, the robot is driven to a small neighborhood of the desired posture, path, or trajectory in finite time. Initial conditions are then discussed considering curvature constraints.

A. Lyapunov based control design

Lyapunov based techniques are used in Theorem 1 to derive a motion controller driving the robot along the *path manifold* to the origin of the error coordinates. Similar to sliding mode control techniques, a state feedback control law is derived to steer the system (1) to the *path manifold* (4) where z_1=0 and z_2=0 by denoting,

$$z_1 = e - \sqrt{2}r\eta,\ z_2 = \theta + \alpha\,. \tag{6}$$

Once the robot reaches the *path manifold*, the *path manifold* guarantees stabilization of the robot to the origin of the error coordinates.

Theorem 1 The following control law asymptotically converges z_1, z_2, and states in $M=\{(e,\theta,\alpha)\in R^3 | e>0\}$ to zero,

$$v = k_1 \tanh z_1 + v_r \cos\theta \tag{7}$$

$$\dot{\phi} = \kappa v = k_2 \tanh z_2 + 2\dot{\theta} + \dot{\phi}_r\ , \tag{8}$$

where k_1 and k_2 are positive control gains that determine maximum convergence rates.

Proof: First, define quadratic Lyapunov candidate functions,

$$V = V_1 + V_2\ ;\quad V_1 \equiv \frac{1}{2}{z_1}^2,\ V_2 \equiv \frac{1}{2}{z_2}^2\,. \tag{9}$$

Applying (7) and (8), the time derivatives of V_1 and V_2 are then,

$$\dot{V}_1 = z_1\dot{z}_1 = -k_1 z_1 \tanh(z_1) + z_1 f(e,\theta,\alpha) \tag{10}$$

$$\dot{V}_2 = z_2\dot{z}_2 = z_2(2\dot{\theta} + \dot{\phi}_r - \dot{\phi}) = -k_2 z_2 \tanh\left(z_2\right) \le 0\,, \tag{11}$$

where $f = v\left(1-\cos(\alpha)\right) - \dfrac{r\sqrt{2}\sin(2\theta)}{\eta}\dot{\theta}$.

Since $\dot{V}_2$ is negative definite, $z_2 \to 0$ (i.e., $\alpha+\theta \to 0$) as $t \to \infty$. Further, α and θ asymptotically converge to zero simultaneously by the controller (8) (see Corollary 1 in Appendix) such that $f \to 0$. Thus, $\dot{V}_1$ converges to a negative definite function, $-k_1 z_1 \tanh(z_1)$, which drives z_1 to zero. Since $z_1 \to 0$, $z_2 \to 0$, and $\alpha \to -\theta \to 0$ as $t \to \infty$, we finally have $e \to \sqrt{2}r\eta \to 0$ as $t \to \infty$ per (6). ■

Further, exponential local convergence is achieved in a small neighborhood of the equilibrium point (see Corollary 2 in Appendix). Notice that *tanh* functions are implemented to resolve the common problem of excessive velocity commands given large initial conditions.

To summarize, by applying the controller (7) and (8) to the system (1), we have $(e,\theta,\alpha) \to (0,0,0)$, $(\dot{e},\dot{\theta},\dot{\alpha}) \to (0,0,0)$, $v \to v_r$, and $\dot{\phi} \to \dot{\phi}_r$ (i.e. $\kappa \to \kappa_r$) as $t \to \infty$, which assures tracking, regulation, and path following capability.

B. Dependence on Initial Conditions

Due to fundamental path geometry constraints, allowable initial conditions must be considered to assure that curvature bounds are satisfied during convergence to the *path manifold*. Initial conditions are divided into three zones, Fig. 4, based upon the *path manifold* using r=1/κ_{max}. Zone 3 is the interior of the circle defined by κ_{max} and the path must violate curvature constraints in order to asymptotically converge to the *path manifold*. Note that the robot cannot compensate for distance errors for $z_1(0)$=0 in posture regulation where v_r=0 since we have v=0 per (7). Thus, $z_1(0)$>0 is necessary to ensure forward motion and satisfy the curvature constraint of the actual robot during convergence to the *path manifold*. In Zone 2, the curvature constraint is violated for certain initial orientations due to limited steering space. To be guaranteed to satisfy curvature constraints for any initial orientation, the robot must start in Zone 1. Further, the issue of initial conditions found in Zones 2 and 3 can be resolved easily by commanding the robot to move into Zone 1 using intermediate goal postures.

VI. Controller Evaluation

A. Methods and Procedures

Simulations are used to validate the controller's capability to satisfy curvature and velocity constraints. We use v_{max}=0.5 *m/s* and κ_{max}=3 m^{-1} for physical constraints. Control gains are then determined to satisfy physical constraints similarly to

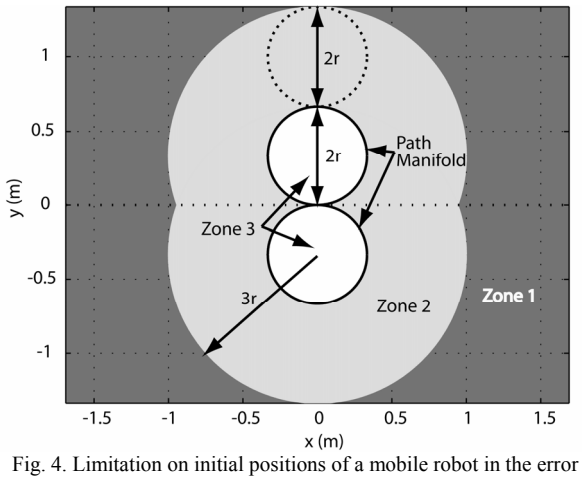

Fig. 4. Limitation on initial positions of a mobile robot in the error coordinates based upon maximum path curvature, r=1/κ_{max}=0.34 *m*.

[2]; $k_1=v_{max}-v_{des}$ and $k_2=(v_{max}\kappa_{max}-v_{des}\kappa_{des})\tanh(1/z_1(0))$. Since initial values of v and κ specified by (7) and (8) rarely match those of the robot, the controller dynamics are extended in a cascade fashion per Bacciotti Theorem 19.2 [15].

Simulation results of posture regulation and trajectory tracking are presented here since they are more common and difficult problems. Since reference path or trajectory generation is not the focus of this research, we implement typical simple paths with constant curvature [12] for trajectory tracking; $\dot{x}_r = v_{des}\cos(\phi_r(t))$, $\dot{y}_r = v_{des}\sin(\phi_r(t))$, and $\dot{\phi}_r(t) = v_{des}\kappa_{des}$ where $x_r(0)= y_r(0)= 0$ *m*. Note that path following uses a time independent reference path whereas a path in trajectory tracking is time dependent as mentioned in Sec. III. Thus, trajectory tracking can easily solve path following modifying references. It is also worth while to note that in path following path convergence is typically slower and velocity commands are lower compared to trajectory tracking.

B. Results and Discussion

Posture regulation is shown in Fig. 5 and eight different initial orientations with $e(0)=2$ *m* are considered. These results show that trajectory paths are smooth and only forward velocity is required. Note that these trajectory paths are symmetric with respect to the *x*-axis since our *path manifold* is so as mentioned in IV. In order to illustrate states and control inputs, we choose a worst case, $\theta(0)=\pi$, where largest control inputs are commanded among given initial conditions. Fig. 5 (b) shows that z_2 converges to zero asymptotically and quickly. As a result, all other states simultaneously reach to a small neighborhood of the origin in finite time as proven in Theorem 1 and Corollary 1. Fig. 5 (c) also verifies that velocity and curvature commands satisfy our physical constraints, $v_{max}=0.5$ *m/s* and $\kappa_{max}=3$ m^{-1}.

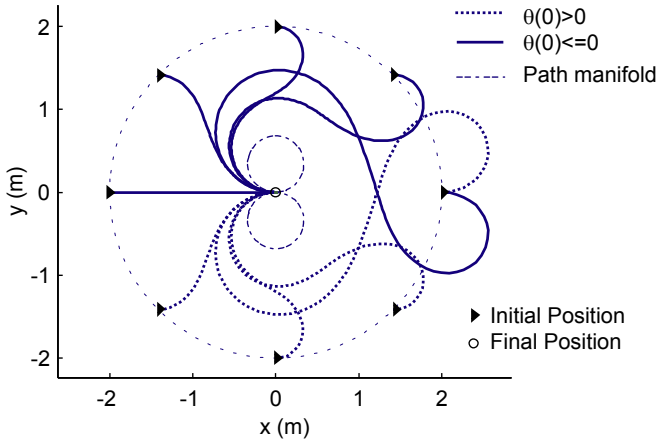

(a) Trajectory paths of posture regulation

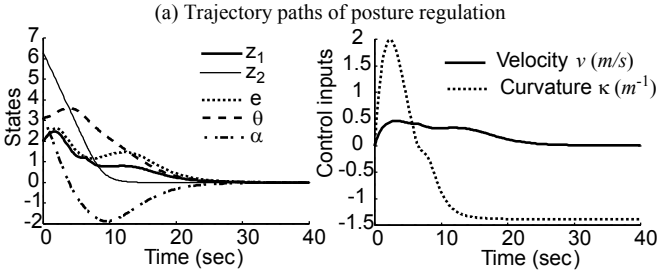

(b) States $\theta(0)=\pi$ *rad* (c) Control inputs $\theta(0)=\pi$ *rad*

Fig. 5. Posture regulation, IC: $e(0)=2$ *m*, $\theta(0)=\alpha(0)=\pm n\pi/4$ *rad* (n=0,1,2,3,4).

Similarly, Fig. 6 shows trajectory paths, states, and control inputs in trajectory tracking for three different initial conditions: Q_1, Q_2, and Q_3. These results also verify that all states converge to zero as designed. Velocity and curvature commands are well bounded and track reference commands. Similar to [2], the proposed controller can easily be implemented on actual robots, and controller performance in simulation and experiment is almost similar given a high traction surface such as carpet. Further, future work should focus on planning reference paths and trajectories in order to consider available steering space and obstacles in real environments.

VII. Conclusions

A new kinematic motion controller is derived using a circular *path manifold* and Lyapunov based techniques. Allowable initial conditions are estimated considering curvature limitations. The proposed controller solves primary motion control problems while satisfying physical constraints given allowable initial conditions. Our simulation results verify that control inputs are bounded and paths are smooth.

Appendix

Corollary 1 The control law (7) and (8) stabilize the closed loop system to the origin of the polar error coordinate system along the *path manifold*.

Proof: Let $\alpha=(z_3-1)\theta$ where $z_3\in R^1$, we have,

$$z_2= z_3\theta. \tag{12}$$

Differentiating (12) and substituting into (11), we have,

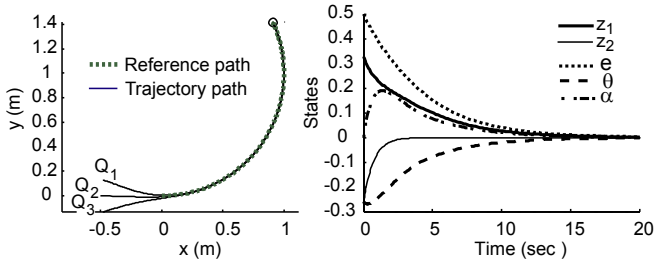

(a) Trajectory paths (b) States for IC Q_1

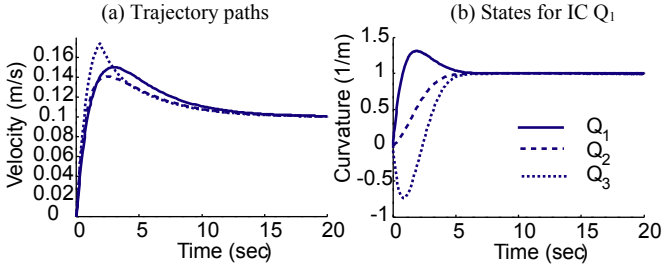

(b) Forward velocity (c) Curvature

Fig. 6. Trajectory Tracking: $v_{des}=0.1$ *m/s*, $\kappa_{des}=1$ m^{-1}, IC [e(0), θ(0), α(0)]:Q_1= [0.5 *m*, -π/12 rad, 0], Q_2 = [0.5 *m*, 0, 0], Q_3= [0.5 *m*, π/12 rad, 0].

$$\dot{V}_2 = z_2(\dot{z}_3\theta + z_3\dot{\theta}) = \theta^2 z_3\dot{z}_3 + z_3^2\theta\dot{\theta} = -k_2 z_2 \tanh(z_2) \le 0 \quad (13)$$

In order to provide a unique equilibrium point, we define $S=\{e>0,\ \theta\in[-\pi,\pi],\ \alpha\in[-\pi,\pi]\} \subset M$. Then, define Lyapunov functions to show the stabilization of θ to zero in S,

$$V_3 = \frac{1}{2}z_3^2,\ V_4 = \frac{1}{2}\theta^2 . \quad (14)$$

First, consider Case *i*) where $\theta\neq 0$ in S where $t\geq 0$. Note that z_2 and θ are bounded such that z_3, $\dot{z}_3$, and $\dot{\theta}$ are bounded according to (11) - (13). Also note that z_2 asymptotically converges to zero by Theorem 1 for any θ and α for $t\geq 0$, and by (12) $z_3=0$ if and only if $z_2=0$ for all $\theta\neq 0$. In order for (13) to be true for any non-zero θ, z_2, and z_3, it must be true that $\dot{V}_3 = z_3\dot{z}_3 < 0$ and $\dot{V}_4 = \theta\dot{\theta} < 0$. Further, since $z_2\to 0$ as $t\to\infty$, it is easily verified that $\dot{V}_3 \to 0^-$ and $\dot{V}_4 \to 0^-$ such that θ and z_3 asymptotically approach zero.

Now consider two other cases where $\theta = 0$. In Case *ii*) where z_3 is bounded (i.e. $|z_3|<\infty$), it must be true from (12) that $z_2=0$ and boundedness of $\dot{z}_3$ is shown by (13). As a results we have $\theta^2 z_3\dot{z}_3 = 0$. Thus, (13) becomes $z_3^2\theta\dot{\theta} = -k_2 z_2 \tanh(z_2)$, which can be rewritten as,

$$\dot{V}_4 = \theta\dot{\theta} = \frac{-k_2 z_2 \tanh(z_2)}{z_3^2} = \frac{-k_2\theta^2 \tanh(z_2)}{z_2} \quad (15)$$

Applying $z_2=0$ and $\theta=0$ to (15), by L'Hopital's rule, we have,

$$\dot{V}_4\Big|_{\substack{\theta=0\\ z_2=0}} = -k_2\theta^2\Big|_{\theta=0} \cdot \lim_{z_2\to 0}\frac{\tanh(z_2)}{z_2} = -k_2\theta^2\Big|_{\theta=0} = 0 \quad (16)$$

Further, in Case *iii*) consider $\theta = 0$ and unbounded z_3 (i.e. $z_3=\pm\infty$), it is verified that $\theta^2 z_3\dot{z}_3$ and $z_3^2\theta\dot{\theta}$ must be bounded to satisfy (13). As a result, in conjunction with Case *ii*), $\dot{V}_4 = \theta\dot{\theta} = 0$ must always be true when $\theta=0$. Summarizing the aforementioned cases, it is shown that $\dot{V}_4 < 0$ for $\theta\neq 0$ and $\dot{V}_4 = 0$ for $\theta = 0$. This proves that θ asymptotically converges to zero as $t\to\infty$. ■

Corollary 2 The origin of the closed loop system is locally exponentially stable by the control law (7) and (8).

Proof: The controller (8) drives $\alpha\to -\theta$ by Theorem 1 such that the system (1) becomes,

$$\begin{aligned}\dot{e} &= (-v + v_r)\cos\theta \\ \dot{\theta} &= -\dot{\alpha} = -(v + v_r)\frac{\sin\theta}{e} - \dot{\phi}_r\end{aligned} . \quad (17)$$

The following must be true near the equilibrium point per (17),

$$v \to v_r,\ e \to -\frac{2v_r}{\dot{\phi}_r}\sin\theta . \quad (18)$$

Applying (18) to the control law (7) and (8), and linearizing near the origin, we have,

$$\begin{aligned} v &= k_1 e + v_r \\ \dot{\phi} &= k_2(\theta + \alpha) + 2k_1\alpha + \dot{\phi}_r . \end{aligned} \quad (19)$$

Further, applying (19) to (1) and linearizing, we then have,

$$\begin{aligned} \dot{e} &= -k_1 e \\ \dot{\theta} &= k_1\alpha = -k_1\theta \\ \dot{\alpha} &= -k_2\theta - (k_1 + k_2)\alpha = -k_1\alpha \end{aligned} , \quad (20)$$

which proves that the control law provides local exponential stability if $k_1>0$. ■

REFERENCES

[1] X. Zhu, Y. Kim, and M. A. Minor, "Cooperative distributed robust control of modular mobile robots with bounded curvature and velocity," *in Proc. IEEE/ASME Int. Conf. Advanced Intelligent Mechatronics*, Monterey, CA, United States, pp. 1151-1157, 2005.

[2] Y. Kim and M. A. Minor, "Path manifold-based kinematic control of wheeled mobile robot considering physical constraints," *International Journal of Robotics Research*, vol. 26, pp. 955-975, 2007.

[3] C. Samson, "Time-varying feedback stabilization of car-like wheeled mobile robots," *Int. Journal of Robotics Research*, vol. 12, pp. 55-64, 1993.

[4] A. Tayebi, M. Tadjine, and A. Rachid, "Path-following and point-stabilization control laws for a wheeled mobile robot," *in Proc. UKACC Int. Conf. Control*, Exeter, UK, pp. 878-883, 1996.

[5] R. W. Brockett, "Asymptotic stability and feedback stabilization," *in R. W. Brockett, R. S. Millman, and H. J. Sussmann, editors, Differential Geometric Control Theory, volume 27 of Progress in Mathematics*, Birkhauser, Boston, pp. 181-191, 1983.

[6] A. Astolfi, "On the stabilization of nonholonomic systems," *in Proc. IEEE Conf. Decision and Control*, New York, NY, USA, pp. 3481-6 vol.4, 1994.

[7] M. Aicardi, G. Casalino, A. Bicchi, and A. Balestrino, "Closed loop steering of unicycle like vehicles via Lyapunov techniques," *IEEE Robotics & Automation Magazine*, vol. 2, pp. 27-35, 1995.

[8] A. Astolfi, "Exponential stabilization of a wheeled mobile robot via discontinuous control," *Trans. the ASME. Journal of Dynamic Systems, Measurement and Control*, vol. 121, pp. 121-7, 1999.

[9] M. A. Minor, B. W. Albiston, and C. L. Swensen, "Simplified Motion Control of a Two Axle Compliant Framed Wheeled Mobile Robot," *IEEE Trans. Robotics*, vol. 22, pp. 491-506, 2006.

[10] G. Indiveri, "Kinematic time-invariant control of a 2D nonholonomic vehicle," *in Proc. IEEE int. Conf. Decision and Control*, Phoenix, AZ, USA, pp. 2112-17, 1999.

[11] R. Siegwart and I. R. Nourbakhsh, *Introduction to autonomous mobile robots*: MIT Press, Cambridge, MA, 2004.

[12] J. A. Reeds and L. A. Shepp, "Optimal paths for a car that goes both forwards and backwards," *Pacific Journal of Mathematics*, vol. 145 no. 2, pp. 367-393, 1990.

[13] D. Chwa, "Sliding-Mode Tracking Control of Nonholonomic Wheeled Mobile Robots in Polar Coordinates," *IEEE Trans. Control Systems Technology*, vol. 12, pp. 637-644, 2004.

[14] J. Guldner and V. I. Utkin, "Sliding mode control for an obstacle avoidance strategy based on an harmonic potential field," *in Proc. IEEE Conf. Decision and Control*, San Antonio, TX, USA, pp. 424-9, 1993.

[15] A. Bacciotti, *Local stabilizability of nonlinear control systems*, vol. 8: World Scientific, Singapore, 1991.